

Formation and Evolution of Protoplanetary Disks: Observations and Modeling of Jets, Disks, and Disk Substructures

Laura M. Pérez

Universidad de Chile, Departamento de Astronomía,
Camino El Observatorio 1515, Las Condes, Santiago, Chile
email: lperez@das.uchile.cl

Abstract. Planet formation takes place in the gaseous and dusty disks that surround young stars, known as protoplanetary disks. With the advent of sensitive observations and together with developments in theory, our field is making rapid progress in understanding how the evolution of protoplanetary disks takes place, from its inception to the end result of a fully-formed planetary system. In this review, I discuss how observations that trace both the dust and gas components of these systems inform us about their evolution, mass budget, and chemistry. Particularly, the process of disk evolution and planet formation will leave an imprint on the distribution of solid particles at different locations in a protoplanetary disk, and I focus on recent observational results at high angular resolution in the sub-millimeter regime, which have revealed a variety of substructures present in these objects.

Keywords. stars: formation, planetary systems: protoplanetary disks, instrumentation: high angular resolution, instrumentation: interferometers

1. Introduction

Our current view of the process of low-mass star and planet formation is that they occur simultaneously. When protostars are born, they are generally surrounded by circumstellar material whose geometry is envelope-like in the earliest phases of formation, and later becomes disk-like once the envelope is dissipated. Planets are formed out of the same circumstellar material that feeds the protostar, and we generally refer to these planet-forming disks as protoplanetary disks (Williams & Cieza 2011). Eventually, the protostar will reach the main-sequence, perhaps surrounded by a planetary system, while the leftover material from this process may be observed as a debris disk. In the following, I discuss recent ALMA results related to the earliest stages of star formation, when jets and outflows are still present, then I discuss what ALMA observations tells us about the evolution of solids in protoplanetary disks, and finally I present new results on disk substructures observed at high angular resolution with ALMA.

2. Outflows and jets

Jets and outflows become part of the picture in the early stages of the process, playing an important role: they extract excess angular momentum during the protostellar collapse, allowing for accretion of material onto the forming protostar. Outflows/jets are present across a wide range of stellar masses, from low to high-mass stars, and they have an impact over different physical scales: from the disk to the envelope, and all the way

to cloud scales (e.g. [Aso et al. 2015](#), [Yusef-Zadeh et al. 2017](#)). ALMA observations in dust continuum and molecular lines can trace the outflow ([Louvet et al. 2018](#)) or the jet ([Lee et al. 2017](#)) from young protostars, constraining the launching radii to be quite small. In the case of the edge-on low-mass star HH 330 ([Louvet et al. 2018](#)) the morphology and kinematics is consistent with a slow disk wind launching at radii $< 7\text{au}$. These observations also reject the wide binary hypothesis that was used to explain the wiggling of the optical jet. For HH 212, [Lee et al. \(2017\)](#) are able to measure the rotation of the jet down to 10au from the protostar, inferring a $\sim 0.05\text{au}$ launching radius.

Another important aspect of protostellar evolution, which can be traced with detailed studies of outflows/jets, is how accretion proceeds. Nascent stars are not continuously fed material from the disk but rather have time-variable accretion. It is only recently that theory can be put to the test via observations of jets whose knotty structure may be a signature of episodic protostellar accretion. In a recent study, [Vorobyov et al. \(2018\)](#) modeled the accretion history of gravitationally unstable disks and compared the time delay between bursts of luminosity/accretion with the observed episodic ejection, measured as the separation between jet components/knots in the CARMA-7 source studied in [Plunkett et al. \(2015\)](#). Such comparisons are finally testing theoretical predictions against observations.

3. The evolution of solids in disks

Inside the circumstellar disks that generally surround young stars is where the ISM dust is converted into planetary systems. At long radio wavelengths (mm to cm) the dust thermal emission mainly arises from macroscopic particles (“pebbles”) and thus, observations at this wavelength regime allow for the last direct detection of solids before we can study the end product, planetary systems. Surveys of young star-forming regions have provided an overview of disk evolution, allowing for the comparison with host properties, environment, and age. From IR-excess studies, we know that disk lifetimes are short ([Hernández et al. 2007](#)) but only recently we have directly observed the evolution of disk mass with time from mm-wave observations ([Ansdell et al. 2016](#), [Pascucci et al. 2016](#), [Barenfeld et al. 2016](#)), where the oldest star-forming regions appear to have a larger fraction of lower-mass disks than the younger ones (albeit caveats remain regarding sample completeness, [Cieza et al. 2019](#)). In any case, grain growth, fragmentation, and the radial drift of macroscopic particles will have an impact on the observed solid mass, and the last two particularly become barriers to the planet formation process (see, e.g. [Testi et al. 2014](#)). A way to test for the evolution of solids in disks and the presence of these barriers is by inferring their particle-size distribution from multi-wavelength observations. In a few examples we know that there is a radial segregation by particle size, either from constraints on disk size with wavelength (e.g. [Tripathi et al. 2018](#)) or from the observed variations of the opacity spectral index with radial distance from the star (e.g. [Tazzari et al. 2016](#)). However, nature somehow must overcome these barriers and perhaps a way to promote solid agglomeration and support the planet formation process is by the presence of substructure, since a disk with substructure will concentrate solids needed for planetesimal formation (e.g. [Pinilla et al. 2015](#), [Birnstiel et al. 2013](#)). Substructure can be naturally generated via instabilities in the disk, for example large-scale gravitational instabilities (e.g., [Dipierro et al. 2015](#)), zonal flows (e.g., [Johansen et al. 2009](#)), or hydrodynamical instabilities that can concentrate solids in vortices (e.g., [Zhu & Stone 2014](#)). On the other hand, the presence of companions, either stellar-mass or planet-mass, will also excite substructure in the disk (e.g. [Wolf & D’Angelo 2005](#)) that can then trap the solids and promote its concentration. For many disks, we already knew about substructure: this is the case of transition disks, for which the presence of a cavity/gap was

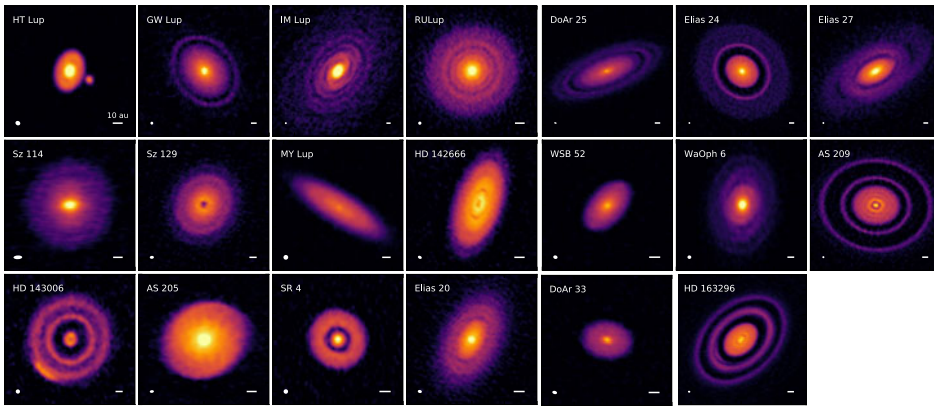


Figure 1. DSHARP observations of the 20 young stars targeted with ALMA high resolution observations at 1.3 mm. Adapted from [Andrews *et al.* \(2018\)](#).

inferred from spectral energy distribution modeling and latter confirmed through imaging (some examples are [Brown *et al.* 2009](#), [Geers *et al.* 2007](#), [Andrews *et al.* 2011](#)). With the advent of ALMA, many disks have been targeted with sufficient angular resolution to reveal a whole variety of substructures: gaps and rings, sometimes with asymmetries, and sometimes with spirals (e.g. [Fukagawa *et al.* 2013](#), [Pérez *et al.* 2014](#), [ALMA Partnership *et al.* 2015](#), [Tobin *et al.* 2016](#), [Pérez *et al.* 2016](#), [Dong *et al.* 2018](#)). But to understand the prevalence, statistics, and properties of such features, we needed a larger sample from which to study.

4. DSHARP: Disks Substructures at High Angular Resolution Project

The “Disks Substructures at High Angular Resolution Project” (DSHARP) is an ALMA Large Program devoted to study substructures in protoplanetary disks, through observations of high angular resolution at millimeter wavelengths of a large sample of young stars ([Andrews *et al.* 2018](#)). The focus of the program is on “classical” Class II disks, since transitional disks already have known substructure and debris disks are more evolved objects. We targeted 20 young stars, two of which were multiple systems, and we managed to image 23 protoplanetary disks in ALMA Band 6 (1.3 mm wavelength) with an angular resolution of few au over the full extent of the disk (Figure 1). Both dust continuum emission and a gas tracer (^{12}CO) were targeted. These observations have revealed that substructure appears to be ubiquitous ([Andrews *et al.* 2018](#)) and that the most common type of substructure is concentric rings/gaps ([Huang *et al.* 2018](#)). Rings/gaps can have high and low contrast, can be located close and far from the star, and we find no correlations between the stellar properties and ring properties ([Huang *et al.* 2018](#)). Surprisingly, the second most common type of substructure in this sample was spiral arms ([Huang *et al.* 2018](#)), which appear to be quite diverse as well in terms of their properties around single-star systems. In multiple systems, we find that the substructure observed is evidence of star-companion-disk interactions ([Kurtovic *et al.* 2018](#)). Asymmetries in the disks of this sample were found only in two targets: HD 163296 ([Isella *et al.* 2018](#)) and HD 143006 ([Pérez *et al.* 2018](#), see Figure 2), since the majority of the disks observed had very symmetric dust continuum emission, as beautifully demonstrated for the case of AS 209 ([Guzmán *et al.* 2018](#)). Several of the observed rings appear to be radially narrow compared to the pressure scale height, indicative of dust trapping taking place in these rings ([Dullemond *et al.* 2018](#)). Detailed hydrodynamical simulations

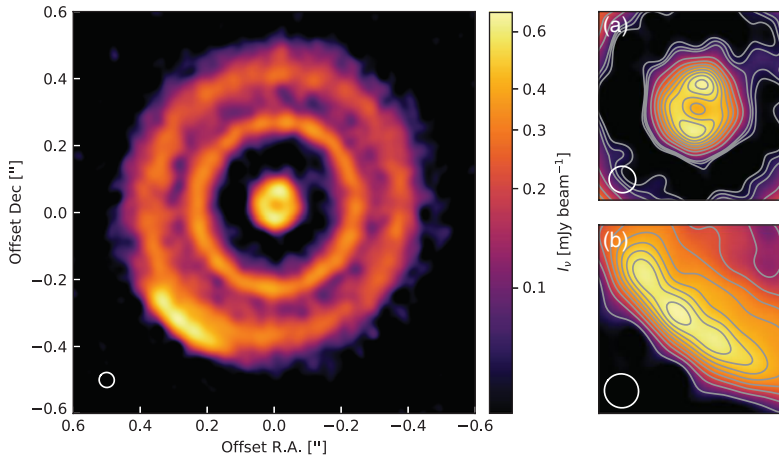


Figure 2. The ALMA view in dust continuum emission of the disk around HD 143006. The left panel shows that the disk resolves into three concentric rings and an arc of emission outside of the outermost ring. The right panels show that the innermost ring connects to the outer disk with a low-surface brightness bridge-like feature (panel (a)), and that the bright arc of emission resolves into further substructure with three peaks roughly separated by 10au (panel (b)). In panel (a), the contours are at 3, 4, 5 σ , then continue being spaced by 5 σ , while in panel (b) the contours start and are spaced by 5 σ . Note that σ is the rms noise of the image ($\sigma = 14.3 \mu\text{Jy beam}^{-1}$). Ellipses in the bottom-left corner of each panel indicate the beam size of $46 \times 45 \text{ mas}$ ($7.6 \times 7.4 \text{ au}$). Adapted from Pérez *et al.* (2018).

show that several of the observed gaps can be explained with the presence of massive planets (Zhang *et al.* 2018). Finally, opacity calculations needed to interpret in terms of mass the rings observed within the DSHARP collaboration are presented in Birnstiel *et al.* (2018). For a full detailed discussion of all these findings see the Focus Issue from ApJ Letters (Andrews *et al.* 2018, Huang *et al.* 2018, Huang *et al.* 2018, Kurtovic *et al.* 2018, Birnstiel *et al.* 2018, Dullemond *et al.* 2018, Zhang *et al.* 2018, Isella *et al.* 2018, Pérez *et al.* 2018).

5. Observing disk substructures at multiple wavelengths: an example in the T Tauri star HD 143006

Multi-wavelength observations of disks at high spatial resolution can provide critical constraints on the structure and distribution of solids and gas in protoplanetary disks (e.g. Cazzoletti *et al.* 2018). In particular, scattered-light imaging observations are critical as they trace the disk surface layer, they critically depend on the disk structure and stellar parameters, and current instruments can provide high angular resolution images (e.g. SPHERE, GPI, SCExAO, NACO). As an example of what can we learn from studying the same object at multiple wavelengths, we discuss the case of HD 143006, a G7 spectral type young star at a distance of $165 \pm 5 \text{ pc}$ (Gaia Collaboration *et al.* 2018), with a mass between 1.5-2.0 M_{\odot} , and age between 4 – 12 Myr old (Andrews *et al.* 2018). Benisty *et al.* (2018) analyzed SPHERE J-band polarized intensity imaging of this star at 40 mas resolution, which shows a strong East-West asymmetry in scattered light, with the East side of the disk being brighter than the West. They show through hydrodynamic simulations and radiative transfer, that a moderately misaligned inner disk (misalignment $< 30^{\circ}$) can reproduce the set of narrow shadows in the innermost bright ring observed in scattered light, together with the East-West broad shadow observed in the entire disk. Thus, shadows in scattered light can be a different probe of disk substructure, as scattered light observations are very sensitive to the illumination pattern. However, scattered

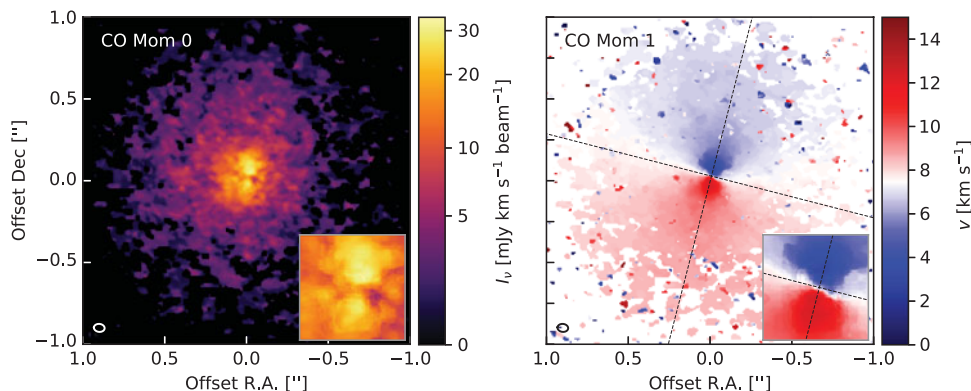


Figure 3. The ALMA view in ^{12}CO gas emission of the disk around HD 143006. The left panel shows the integrated intensity of the $^{12}\text{CO}(2-1)$, also known as moment 0 map. In this particular line tracer there is no clear disk substructure, except for depleted CO emission in the inner disk close to the central star. The right panel shows the velocity field of the CO line, which follows a Keplerian pattern except for the inner disk close to the central star, where the position angle and inclination of the disk appear to change, as revealed by further modeling. Ellipses in the bottom-left corner of each panel indicate the beam size of 66×49 mas (11×8 au). Adapted from Pérez *et al.* (2018).

light imaging cannot probe the inner disk directly, due to the inner working angle of such observations (80 mas for SPHERE) that does not allow for a clear view of the inner disk misalignment.

As part of DSHARP, new ALMA observations of HD 143006 at high angular resolution provided new information about the kinematics of the protoplanetary disk, as well as the substructure in gas and dust (Pérez *et al.* 2018). In the dust continuum emission the disk resolved into three concentric rings, a large arc with three bright peaks outside of the outermost ring, and a bridge-like emission feature detected between the inner and middle ring (see Figure 2). In gas emission, the disk extends to a factor of two larger radii, with no obvious asymmetries or rings detected, although the inner disk appears depleted of emission as in the dust continuum map (see Figure 3). Modeling of the kinematics indicated that a single geometry (inclination, position angle) for the disk cannot reproduce the Keplerian rotation pattern, suggesting a misalignment between the inner disk and the outer disk. Detailed modeling of the dust continuum visibilities obtained by ALMA revealed the actual degree of misalignment: either a $< 10^\circ$ misalignment if the near side of the disk is the same for the inner and outer disk, or a moderate $\sim 40^\circ$ misalignment if the inner and outer disk have opposite near sides. Further hydrodynamical modeling by Zhang *et al.* (2018) suggest that a massive planet of $10 - 20 M_{\text{Jup}}$ could create a gap between the inner and outer disk and radially segregate the large and small dust grains traced by the ALMA and SPHERE observations.

6. Future

The study of the formation and evolution of protoplanetary disks will likely continue to tackle the topic of substructures and what is their origin. On one hand, future studies that trace the chemistry of disks during planet formation will be a fundamental piece of the puzzle, for which ALMA is perfectly suited. On the other hand, tracing the embedded planets that perhaps are the cause of the observed substructure will be fundamental to understand the origin of the observed features in disks. Future studies with ALMA, VLT, and next-generation instruments like the E-ELT, SKA, and ng-VLA should advance our knowledge on protoplanetary disks and planet formation.

References

- ALMA Partnership, Brogan, C. L., Pérez, L. M., *et al.* 2015, *ApJ*, 808, L3
- Andrews, S. M., Huang, J., Pérez, L. M., *et al.* 2018, *ApJ*, 869, L41
- Andrews, S. M., Wilner, D. J., Espaillat, C., *et al.* 2011, *ApJ*, 732, 42
- Ansdell, M., Williams, J. P., van der Marel, N., *et al.* 2016, *ApJ*, 828, 46
- Aso, Y., Ohashi, N., Saigo, K., *et al.* 2015, *ApJ*, 812, 27
- Barenfeld, S. A., Carpenter, J. M., Ricci, L., *et al.* 2016, *ApJ*, 827, 142
- Benisty, M., Juhász, A., Facchini, S., *et al.* 2018, *A&A*, 619, A171
- Birnstiel, T., Dullemond, C. P., & Pinilla, P. 2013, *A&A*, 550, L8
- Birnstiel, T., Dullemond, C. P., Zhu, Z., *et al.* 2018, *ApJ*, 869, L45
- Brown, J. M., Blake, G. A., Qi, C., *et al.* 2009, *ApJ*, 704, 496
- Cazzoletti, P., van Dishoeck, E. F., Pinilla, P., *et al.* 2018, *A&A*, 619, A161
- Cieza, L. A., Ruíz-Rodríguez, D., Hales, A., *et al.* 2019, *MNRAS*, 482, 698
- Dipierro, G., Pinilla, P., Lodato, G., *et al.* 2015, *MNRAS*, 451, 974
- Dong, R., Liu, S.-yuan., Eisner, J., *et al.* 2018, *ApJ*, 860, 124
- Dullemond, C. P., Birnstiel, T., Huang, J., *et al.* 2018, *ApJ*, 869, L46
- Fukagawa, M., Tsukagoshi, T., Momose, M., *et al.* 2013, *PASJ*, 65, L14
- Gaia Collaboration, Brown, A. G. A., Vallenari, A., *et al.* 2018, *A&A*, 616, A1
- Geers, V. C., Pontoppidan, K. M., van Dishoeck, E. F., *et al.* 2007, *A&A*, 469, L35
- Guzmán, V. V., Huang, J., Andrews, S. M., *et al.* 2018, *ApJ*, 869, L48
- Hernández, J., Hartmann, L., Megeath, T., *et al.* 2007, *ApJ*, 662, 1067
- Huang, J., Andrews, S. M., Dullemond, C. P., *et al.* 2018, *ApJ*, 869, L42
- Huang, J., Andrews, S. M., Pérez, L. M., *et al.* 2018, *ApJ*, 869, L43
- Isella, A., Huang, J., Andrews, S. M., *et al.* 2018, *ApJ*, 869, L49
- Johansen, A., Youdin, A., & Klahr, H. 2009, *ApJ*, 697, 1269
- Kurtovic, N. T., Pérez, L. M., Benisty, M., *et al.* 2018, *ApJ*, 869, L44
- Lee, C.-F., Ho, P. T. P., Li, Z.-Y., *et al.* 2017, *Nature Astron.*, 1, 152
- Louvet, F., Dougados, C., Cabrit, S., *et al.* 2018, *A&A*, 618, A120
- Pascucci, I., Testi, L., Herczeg, G. J., *et al.* 2016, *ApJ*, 831, 125
- Pérez, L. M., Isella, A., Carpenter, J. M., *et al.* 2014, *ApJ*, 783, L13
- Pérez, L. M., Carpenter, J. M., Andrews, S. M., *et al.* 2016, *Science*, 353, 1519
- Pérez, L. M., Benisty, M., Andrews, S. M., *et al.* 2018, *ApJ*, 869, L50
- Pinilla, P., van der Marel, N., Pérez, L. M., *et al.* 2015, *A&A*, 584, A16
- Plunkett, A. L., Arce, H. G., Mardones, D., *et al.* 2015, *Nature*, 527, 70
- Tazzari, M., Testi, L., Ercolano, B., *et al.* 2016, *A&A*, 588, A53
- Testi, L., Birnstiel, T., Ricci, L., *et al.* 2014, *Protostars and Planets VI*, 339
- Tobin, J. J., Kratter, K. M., Persson, M. V., *et al.* 2016, *Nature*, 538, 483
- Tripathi, A., Andrews, S. M., Birnstiel, T., *et al.* 2018, *ApJ*, 861, 64
- Vorobyov, E. I., Elbakyan, V. G., Plunkett, A. L., *et al.* 2018, *A&A*, 613, A18
- Williams, J. P., & Cieza, L. A. 2011, *Annu. Rev. Astron. Astrophys.*, 49, 67
- Wolf, S., & D'Angelo, G. 2005, *ApJ*, 619, 1114
- Yusef-Zadeh, F., Wardle, M., Kunneriath, D., *et al.* 2017, *ApJ*, 850, L30
- Zhang, S., Zhu, Z., Huang, J., *et al.* 2018, *ApJ*, 869, L47
- Zhu, Z., & Stone, J. M. 2014, *ApJ*, 795, 53